

Article

Investigating K/π Decay Muon Yields Using K/π Yields and a Fast Simulation Method

Zuman Zhang, Sha Li, Ning Yu, Hongge Xu, Yuanmeng Xiong and Kun Liu



Article

Investigating K/π Decay Muon Yields Using K/π Yields and a Fast Simulation Method

Zuman Zhang ^{1,2,3} , Sha Li ¹ , Ning Yu ^{1,2,3}, Hongge Xu ^{1,2,*}, Yuanmeng Xiong ^{1,2} and Kun Liu ^{1,2}

¹ School of Physics and Mechanical Electrical & Engineering, Hubei University of Education, Wuhan 430205, China; zuman.zhang@hue.edu.cn (Z.Z.); lisha@hue.edu.cn (S.L.); ning.yuchina@gmail.com (N.Y.); 15926459464@163.com (Y.X.); 13636116140@163.com (K.L.)

² Institute of Astronomy and High Energy Physics, Hubei University of Education, Wuhan 430205, China

³ Key Laboratory of Quark and Lepton Physics (MOE), Central China Normal University, Wuhan 430079, China

* Correspondence: xuhg@cug.edu.cn

Abstract: In ultra-relativistic heavy-ion collisions, the study of muons from kaon (K) and pion (π) decays provides insights into hadron production and propagation in the Quark-Gluon Plasma (QGP). This paper investigates muon yields from K and π decays in Pb–Pb collisions at $\sqrt{s_{\text{NN}}} = 2.76$ TeV using a fast simulation method. We employ a fast Monte Carlo procedure to estimate muon yields from charged kaons and pions. The simulation involves generating pions and kaons with uniform p_{T} and y distributions, simulating their decay kinematics via PYTHIA, and reweighting to match the physical spectra. Our results show the transverse momentum distributions of muons from K and π decays at forward rapidity ($2.5 < y < 4.0$) for different centrality classes. The systematic uncertainties are primarily from the mid-rapidity charged K/π spectra and rapidity-dependent R_{AA} uncertainties. The muon yields from pion and kaon decays exhibit consistency across centrality classes in the p_{T} range of 3–10 GeV/ c . This study contributes to understanding hadronic interactions and decay kinematics in heavy-ion collisions, offering references for investigating pion and kaon decay channels and hot medium effects.

Keywords: decay muon; quark-gluon plasma



Academic Editor: Iurii Karpenko

Received: 28 March 2025

Revised: 21 May 2025

Accepted: 26 May 2025

Published: 3 June 2025

Citation: Zhang, Z.; Li, S.; Yu, N.; Xu, H.; Xiong, Y.; Liu, K. Investigating K/π Decay Muon Yields Using K/π Yields and a Fast Simulation Method. *Particles* **2025**, *8*, 59. <https://doi.org/10.3390/particles8020059>

Copyright: © 2025 by the authors. Licensee MDPI, Basel, Switzerland. This article is an open access article distributed under the terms and conditions of the Creative Commons Attribution (CC BY) license (<https://creativecommons.org/licenses/by/4.0/>).

1. Introduction

In ultra-relativistic heavy-ion collisions, a strongly interacting deconfined medium of quarks and gluons, known as the Quark–Gluon Plasma (QGP), is created. Experimental evidence for the existence of this extreme state of matter has been observed at both the Relativistic Heavy-Ion Collider (RHIC) [1–4] and the Large Hadron Collider (LHC) [5–9]. The study of QGP properties provides crucial insights into the strong interaction under extreme conditions, offering a deeper understanding of quantum chromodynamics (QCD) in the non-perturbative regime.

The production of hadrons consisting of light flavor quarks (u, d, and s) has been extensively investigated in Pb–Pb collisions at LHC energies [10]. These studies aim to explore QGP dynamics and the subsequent hadronization process. After its formation, QGP expands and cools hydrodynamically, undergoing two distinct freeze-out stages. Chemical freeze-out occurs when inelastic collisions cease, fixing the hadron yields [11,12]. This is followed by the kinetic freeze-out, where elastic collisions also stop, fixing the final

momenta of hadrons. Understanding these stages is essential for deciphering the evolution of the system from a deconfined state to hadronic matter.

ALICE has extensively measured the transverse momentum (p_T) spectra of charged pions, kaons, and protons in pp and Pb–Pb collisions across various centralities [10]. A key observation from these measurements is that, within statistical and systematic uncertainties, the nuclear modification factor remains the same for all three particle species at $p_T > 10 \text{ GeV}/c$. This suggests that high- p_T hadrons experience a similar degree of parton energy loss in the QGP, irrespective of their mass or quark content. Furthermore, ALICE has reported that in different centrality intervals, they enhance the systematic uncertainty of the kaon yields by a factor of approximately two in the p_T region where it is later observed that the peaks of the kaon-to-pion ratios are located [13]. ALICE has also reported that the K/π ratio exhibits an increasing trend from approximately 0.2 to 0.6 as the particle momentum rises to 3 GeV/c , beyond which the ratio approaches a plateau.

Kaons (K) and pions (π) are known to decay into muons with well-defined branching ratios. The decay fraction of charged pions into muons is approximately 1 [14], while for Kaons it is about 0.63 [15]. The study of decay muons originating from K and π can provide complementary information on hadron production and propagation in the medium. Specifically, analyzing the scaling behavior of muon yields from these decays can offer valuable insights into hadronic interactions and decay kinematics.

In this study, we investigate the muon yields from K and π decays in Pb–Pb collisions at a center-of-mass energy per nucleon pair of $\sqrt{s_{NN}} = 2.76 \text{ TeV}$. Our analysis focuses on two parts. First, we employ a fast simulation procedure to estimate the expected muon yields from charged kaons and pions. Second, we examine whether the final charged pion spectra are consistent with the kaon spectra scaled by an appropriate factor within uncertainties. These investigations aim to improve our understanding of hadron decay kinematics and medium effects in heavy-ion collisions.

The paper is structured as follows: In Section 2, we introduce the fast simulation procedure used in our analysis. In Section 3, we describe the centrality rebinning of charged pion and kaon spectra, the transverse momentum distribution of decay muons, the extrapolation of mid-rapidity spectra to forward rapidity, and the generation of muons from charged pion and kaon decays, respectively. In Section 4, we present the results on forward rapidity transverse momentum distributions of muons from K and π decays. Finally, Section 5 provides a summary of our findings and conclusions.

2. Fast Simulation Method

The production of muons from the decays of charged pions and kaons is simulated using a fast Monte Carlo (MC) procedure designed to replicate decay kinematics. This approach leverages extrapolated p_T - and rapidity (y)-dependent spectra of π^\pm and K^\pm as inputs, enabling efficient computation of muon yields. The methodology comprises three principal steps, followed by a systematic propagation of uncertainties:

2.1. Decay Kinematics Simulation

The fast simulation procedure includes the following steps:

1. **Pion and Kaon Generation.** Charged pions and kaons are generated with uniform distributions in p_T and y within predefined ranges ($p_T > 3 \text{ GeV}/c$, $|y| < 6$). This uniform sampling optimizes computational efficiency while ensuring sufficient statistical coverage for rare high- p_T particles. The absence of p_T - or y -dependent weighting at this stage simplifies event generation.
2. **Reweighting to Physical Spectra.** The generated charged pions and kaons are reweighted to match the experimentally measured p_T - and y -extrapolated distri-

butions of π^\pm and K^\pm . For each hadron species, a weight $w(p_T, y)$ is calculated as the ratio of the measured differential yield $d^2N/(dp_T dy)$ to the uniform distribution. Charged pions and kaons are then scaled by these weights, effectively mapping the uniform MC sample onto the physical spectra.

3. Forced Decay via PYTHIA. The decay kinematics of π^\pm and K^\pm into muons are simulated using the PYTHIA 6.4 decayer module [16], which accurately models the momentum distributions of decay products in the parent particle rest frame.

2.2. Uncertainty Propagation

The systematic and statistical uncertainties of the input π^\pm and K^\pm spectra are propagated to the final muon yields through a two-stage procedure:

1. Quadratic Combination of Input Uncertainties. Statistical (σ_{stat}) and systematic (σ_{sys}) uncertainties in the parent hadron spectra are combined in quadrature for each p_T - y bin:

$$\sigma_{\text{total}}(p_T, y) = \sqrt{\sigma_{\text{stat}}^2(p_T, y) + \sigma_{\text{sys}}^2(p_T, y)}. \quad (1)$$

The statistical and systematic uncertainties refer to the experimental uncertainties reported by the ALICE Collaboration. The uncertainty for each p_T - y bin is calculated by combining these statistical and systematic uncertainties in quadrature, as shown in Equation (1). In addition to the uncertainties in the mid-rapidity charged pion and kaon spectra, we have incorporated the systematic uncertainties arising from the rapidity dependence of R_{AA} for charged pions and kaons. Based on the findings of the BRAHMS Collaboration [17] and ATLAS Collaboration [18], we estimate an extra 30% systematic uncertainty for charged pion and kaon spectra to account for this rapidity-dependent R_{AA} effect. The total uncertainty combines both the mid-rapidity charged pion or kaon spectra uncertainties and the rapidity-dependent R_{AA} uncertainties. This total uncertainty defines the upper and lower bounds of the input spectra, which are then propagated to the final muon yields through the simulation process.

2. Monte Carlo Resampling. The fast simulation is repeated twice using the $\pm 1\sigma_{\text{total}}$ -shifted π^\pm and K^\pm spectra as the inputs. The resulting muon yields from these extreme cases define the uncertainty bands for the final predictions.

3. Kaons (K) and Pions (π) Decay Muons

3.1. Centrality Rebin of Charged Pion and Kaon Spectra

The contribution of muons from primary charged pion and kaon decays to the single-muon transverse momentum (p_T) spectrum is estimated using published ALICE measurements of mid-rapidity ($|y| < 0.8$) charged π^\pm and K^\pm yields in Pb–Pb collisions at $\sqrt{s_{\text{NN}}} = 2.76$ TeV [13]. To enhance statistical precision and align with broader centrality classes used in forward muon analyses, the original 0–5% and 5–10% centrality bins are merged into a single 0–10% centrality interval. Similar rebinning is applied to other centrality ranges, resulting in six consolidated classes: 0–10%, 10–20%, 20–40%, 40–60%, 60–80%, and 40–80%.

For each particle species (π^\pm or K^\pm), the differential yields in adjacent centrality bins are combined as follows:

The central value of the merged bin is computed as the arithmetic mean of the yields in the original bins:

$$\left\langle \frac{d^2N}{dp_T dy} \right\rangle_{\text{merged}} = \frac{1}{2} \left(\frac{d^2N}{dp_T dy} \Big|_{\text{bin1}} + \frac{d^2N}{dp_T dy} \Big|_{\text{bin2}} \right). \quad (2)$$

where bin1 and bin2 represent the original centrality intervals (e.g., 0–5% and 5–10%).

Statistical errors (E_{stat}) are combined in following equation:

$$E_{\text{stat,merged}} = \frac{1}{2} \frac{1}{\sqrt{\sigma_{\text{stat,bin1}}^2 + \sigma_{\text{stat,bin2}}^2}}. \quad (3)$$

where $\sigma_{\text{stat,bin1}}^2$ and $\sigma_{\text{stat,bin2}}^2$ represent the statistical uncertainty values in bin1 and bin2, respectively.

Systematic errors (E_{sys}) are combined in quadrature, assuming independence between bins:

$$E_{\text{sys,merged}} = \frac{1}{2} \sqrt{E_{\text{sys,bin1}}^2 + E_{\text{sys,bin2}}^2}. \quad (4)$$

where $E_{\text{sys,bin1}}^2$ and $E_{\text{sys,bin2}}^2$ represent the systematic error values in bin1 and bin2, respectively.

Figure 1 summarizes the rebinned charged pion (upper panel) and kaon (lower panel) p_{T} spectra in the rapidity range $|y| < 0.8$ for centrality classes 0–10%, 10–20%, 20–40%, 40–60%, 60–80%, and 40–80%.

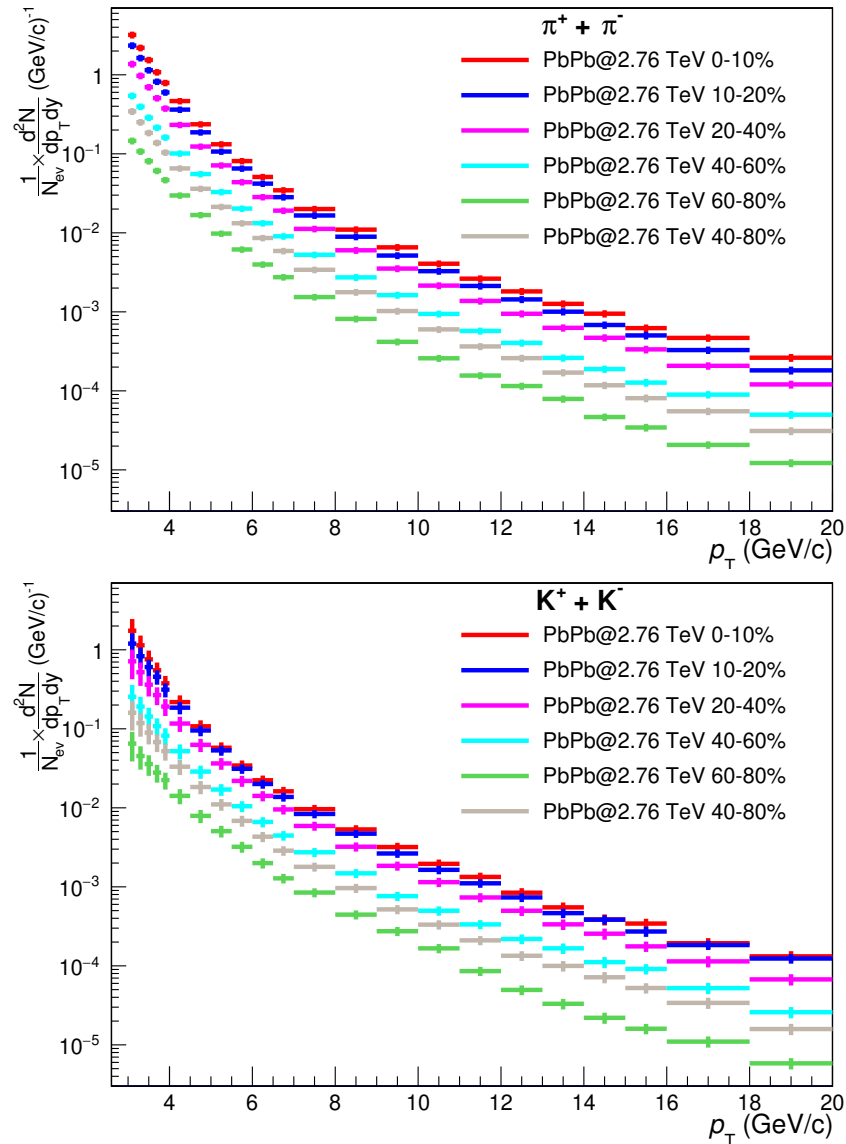


Figure 1. Charged pions measured at mid-rapidity (**upper**) and charged kaons measured at mid-rapidity (**lower**) in Pb–Pb collisions at $\sqrt{s_{\text{NN}}} = 2.76$ TeV in $-0.8 < y < 0.8$ [13]. The statistical errors are plotted as color vertical error bars.

3.2. Rapidity Extrapolation of Charged Pions and Kaons

The extrapolation of rapidity distributions for charged pions (π^\pm) and kaons (K^\pm) is performed using a data-driven approach, incorporating Monte Carlo (MC) simulations. If we previously assumed that R_{AA} is independent of rapidity, the differential yield of these particles as a function of transverse momentum (p_T) and rapidity (y) is expressed as follows:

$$\left[\frac{d^2N^{\pi^\pm(\kappa^\pm)}}{dp_T dy} \right]_{AA} = \langle N_{coll} \rangle \cdot \left[R_{AA}^{\pi^\pm(\kappa^\pm)} \right] \cdot \left[F_{\text{extrap}}^{\pi^\pm(\kappa^\pm)}(p_T, y) \right]_{pp} \cdot \left[\frac{d^2N^{\pi^\pm(\kappa^\pm)}}{dp_T dy} \right]_{pp}^{\text{mid}-y}, \quad (5)$$

$$\left[\frac{d^2N^{\pi^\pm(\kappa^\pm)}}{dp_T dy} \right]_{AA} = \left[F_{\text{extrap}}^{\pi^\pm(\kappa^\pm)}(p_T, y) \right]_{pp} \cdot \left[\frac{d^2N^{\pi^\pm(\kappa^\pm)}}{dp_T dy} \right]_{AA}^{\text{mid}-y}, \quad (6)$$

where $F_{\text{extrap}}(p_T, y)$ represents the p_T -dependent rapidity extrapolation factor. This factor accounts for the variation of particle production as a function of rapidity and is essential for extending measurements from mid-rapidity to a broader rapidity range.

The rapidity extrapolation factor, $F_{\text{extrap}}(p_T, y)$, is determined using Monte Carlo simulations generated with the PYTHIA 6 event generator [16]. These simulations provide a theoretical basis for understanding the rapidity dependence of particle production in high-energy collisions.

For transverse momenta $p_T > 3 \text{ GeV}/c$, the rapidity distributions of charged pions and kaons obtained from PYTHIA 6 simulations are fitted using a polynomial function of the form:

$$F_{\text{fit}}(y) = p_1 x^8 + p_2 x^6 + p_3 x^4 + p_4 x^2 + p_5 x + p_6, \quad (7)$$

where x represents the normalized rapidity variable, and p_1, p_2, \dots, p_6 are the fitting parameters extracted from the simulation data. This functional form effectively captures the rapidity dependence of particle yields and ensures a smooth extrapolation beyond the measured rapidity range.

Figure 2 illustrates the polynomial fits to the simulated rapidity distributions for pions and kaons. The extrapolated results obtained from these fits are employed to extend the measured particle yields beyond mid-rapidity.

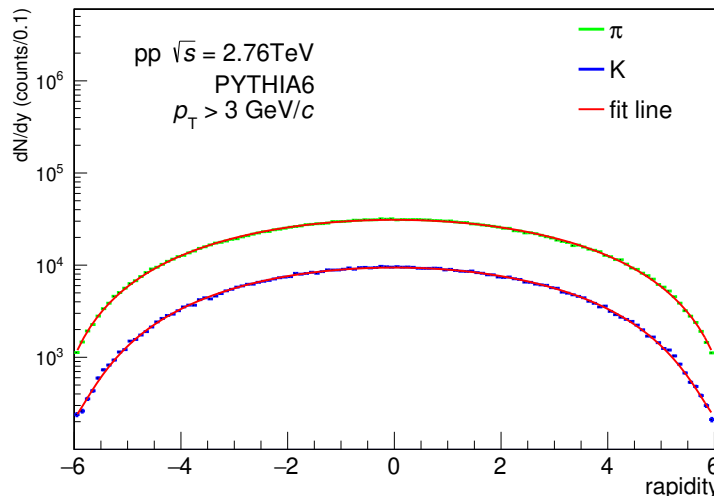


Figure 2. Rapidity distribution of charged (π) and K with ($p_T > 3$) GeV/c from PYTHIA6 and the corresponding polynomial fit.

3.3. Upper Limit of p_T for Charged Pion and Kaon Decay to Muons

The determination of the upper transverse momentum (p_T) limit for charged pions (π^\pm) and kaons (K^\pm) that decay into muons is a crucial aspect of our analysis. The control plots used to establish this upper limit are shown in Figure 3, where the upper panel corresponds to mother pions and the lower panel to mother kaons.

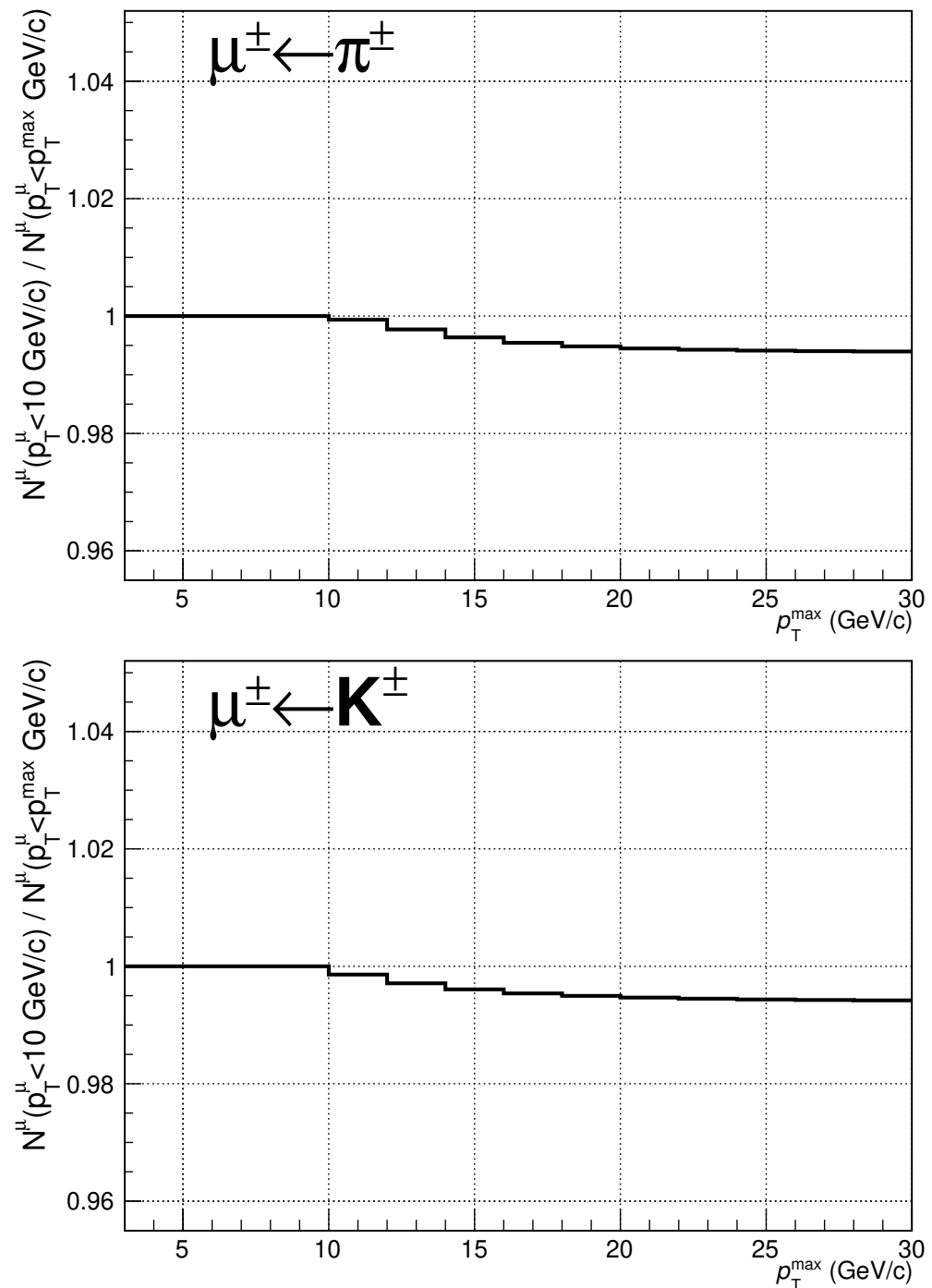


Figure 3. Control plots used to determine the upper limit of p_T for mother pions (**upper** plot) and mother kaons (**lower** plot).

As illustrated in Figure 1, the measured pion and kaon spectra in the ALICE central barrel are limited to $p_T = 20 \text{ GeV}/c$. It is essential to verify whether pions and kaons with $p_T = 20 \text{ GeV}/c$ decay into muons with $p_T < 10 \text{ GeV}/c$.

This verification is performed by analyzing the distributions shown in Figure 3, which present the difference between the number of muons originating from pion and kaon decays with $p_T < 10 \text{ GeV}/c$ and those from pion and kaon decays with $p_T < p_T^{\max}$ as a function of p_T^{\max} .

The results indicate that this difference saturates at $p_T^{\max} = 20 \text{ GeV}/c$, implying that the contributions of pions and kaons with $p_T > 20 \text{ GeV}/c$ to muons with $p_T < 10 \text{ GeV}/c$ can be ignored. This saturation effect confirms that the decay of pions and kaons with $p_T > 20 \text{ GeV}/c$ into muons with $p_T < 10 \text{ GeV}/c$ is negligible.

3.4. Generation of Muons from Charged Pion and Kaon Decay

The study presented in Ref. [19] provides the first measurement of open heavy-flavour production via muons from the semi-leptonic decays of charm and beauty hadrons in Pb–Pb collisions at $\sqrt{s_{NN}} = 2.76 \text{ TeV}$ using the ALICE detector at the LHC. These measurements were conducted in the forward rapidity region ($2.5 < y < 4.0$ [20]), a phase space region uniquely accessible at the LHC by the ALICE experiment in heavy-ion collisions.

Muons originating from the decays of charged pions and kaons in the rapidity range of $2.5 < y < 4.0$ constitute an important background for the measurement of open heavy-flavour production via semi-leptonic decays of charm and beauty hadrons in various collision systems, including pp, p–Pb, Pb–Pb, and Xe–Xe collisions [19,21–23]. Accurately estimating this background is crucial for extracting the heavy-flavour signal with high precision.

In the final step of this analysis, muons from charged pion and kaon decays are simulated using a fast decay kinematics algorithm. The inputs to this simulation include: (1) The rebinned transverse momentum (p_T) spectra of charged pions (upper panel) and kaons (lower panel) in the mid-rapidity region ($|y| < 0.8$), categorized into centrality classes 0–10%, 10–20%, 20–40%, 40–60%, 60–80%, and 40–80%, as described in Section 3.1. (2) The polynomial fits the simulated rapidity distributions of charged pions and kaons, obtained as outlined in Section 3.2.

Using these inputs, the production of muons from charged pion and kaon decays in the forward rapidity range $2.5 < y < 4.0$ is modeled. Additionally, as discussed in Section 3.3, an upper limit of muon $p_T = 10 \text{ GeV}/c$ is applied to the generated muons. In Section 3.3, the upper limit of muon $p_T = 10 \text{ GeV}/c$ is applied to the generated muons, primarily because the measured pion and kaon spectra in the ALICE central barrel are limited to $p_T = 20 \text{ GeV}/c$. The control plots in Figure 3 show that the difference between the number of muons from pion and kaon decays with $p_T < 10 \text{ GeV}/c$ and those from pion and kaon decays with $p_T < p_T^{\max}$ saturates at $p_T^{\max} = 20 \text{ GeV}/c$. This implies that pions and kaons with $p_T > 20 \text{ GeV}/c$ contribute negligibly to muons with $p_T < 10 \text{ GeV}/c$. Therefore, the upper limit of muon $p_T = 10 \text{ GeV}/c$ is set to ignore the contribution of pions and kaons with $p_T > 20 \text{ GeV}/c$ to muons in this p_T range.

4. Results and Discussions

Figure 4 presents the estimated transverse momentum (p_T) distributions of muons originating from the decays of charged pions (black) and kaons (blue) in the rapidity interval of $2.5 < y < 4.0$. The distributions are categorized according to centrality classes: 0–10%, 10–20%, 20–40%, and 40–80%. These results provide crucial input for background estimation in the measurement of open heavy-flavour production via semi-leptonic decays of charm and beauty hadrons.

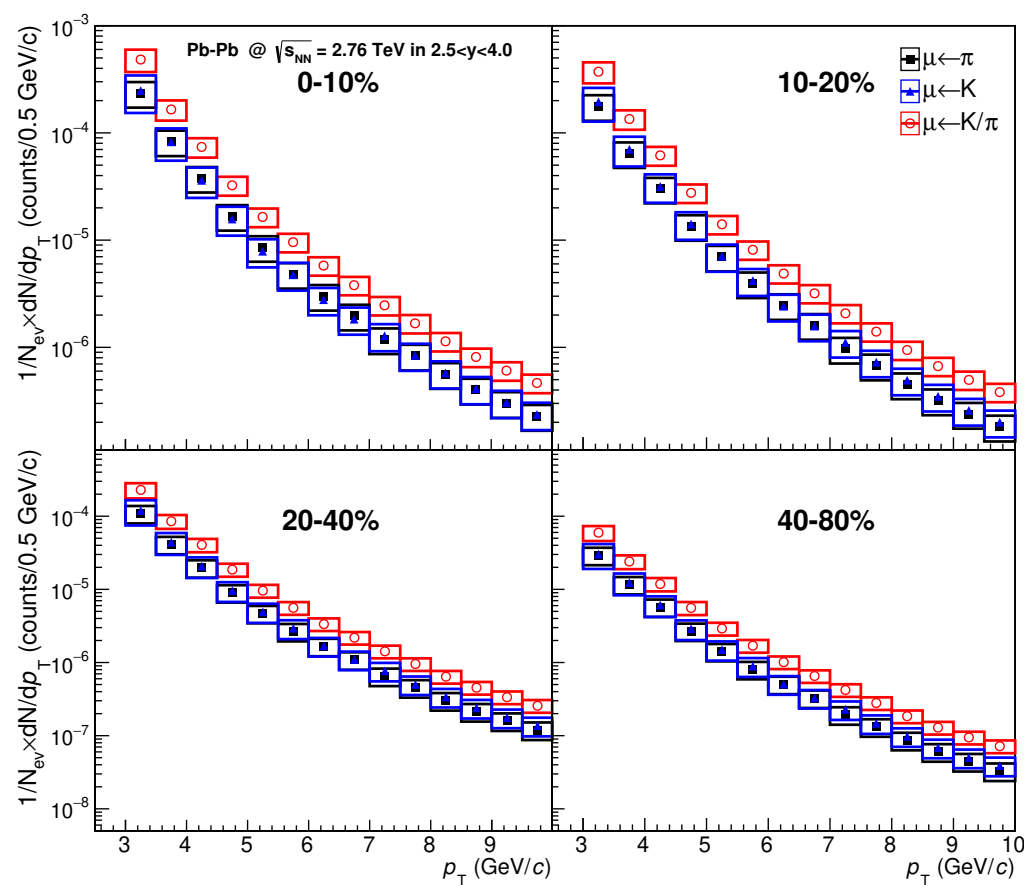


Figure 4. Estimated transverse momentum (p_T) distributions of muons from charged pion (black) and kaon (blue) decays in the rapidity range of $2.5 < y < 4.0$. The distributions are shown for different centrality classes: 0–10%, 10–20%, 20–40%, and 40–80%.

The systematic uncertainties associated with these muon distributions arise primarily from the total uncertainties in the mid-rapidity charged pion and kaon spectra, as discussed in Section 3.1. These uncertainties influence the accuracy of the estimated muon yields in the forward rapidity region.

The p_T distributions of muons originating from charged pion and kaon decays exhibit a high degree of consistency, remaining within uncertainties across all centrality classes, as shown in Figure 4. In particular, the ratio of muons from kaon decay to those from pion decay, relative to the kaon–pion ratio [13] (approximately 0.5), shows an enhancement by about a factor of two.

Furthermore, the scaling behavior of these muon distributions serves as an essential reference for studying pion and kaon decay channels in high-energy heavy-ion collisions. Such analyses contribute to a deeper understanding of hot medium effects and the underlying mechanisms governing hadronic interactions.

5. Summary

In this paper, we have investigated the muon yields from charged kaon (K^\pm) and pion (π^\pm) decays in Pb–Pb collisions at $\sqrt{s_{NN}} = 2.76$ TeV using a fast simulation method. The study aims to improve our understanding of hadron decay kinematics and hot medium effects in heavy-ion collisions.

The fast simulation procedure involves three main steps: generating charged pions and kaons with uniform distributions in transverse momentum (p_T) and rapidity (y), reweighting the charged pion and kaon spectra to match the experimentally measured p_T - and y -dependent spectra of the parent hadrons, and simulating their decay muon kinematics

using PYTHIA 6.4. The systematic uncertainties related to the rapidity dependence of R_{AA} for charged pions and kaons, along with the systematic and statistical uncertainties from the input hadron spectra, are propagated to the final muon yields through a two-stage procedure. We have rebinned the mid-rapidity charged pion and kaon spectra from ALICE measurements into broader centrality classes to enhance the statistical precision. The rapidity distributions of these hadrons are extrapolated using a data-driven approach with polynomial fits to the PYTHIA 6 simulation results. As discussed in Section 3.3, an upper limit of muon $p_T = 10 \text{ GeV}/c$ is applied to the generated muons.

The estimated transverse momentum distributions of muons from charged pion and kaon decays in the forward rapidity region ($2.5 < y < 4.0$) show a high degree of consistency across different centrality classes. These results provide a crucial input for background estimation in the measurement of open heavy-flavour production via semi-leptonic decays of charm and beauty hadrons. While muons from charged pion and kaon decays are produced outside the hot medium, their yields and momentum distributions can indirectly reflect the parent hadrons' production characteristics, which can be influenced by the medium. Moreover, this study contributes to understanding hadronic interactions and decay kinematics in heavy-ion collisions, offering references for investigating pion and kaon decay channels and hot medium effects.

Author Contributions: Methodology, N.Y.; Software, Z.Z. and S.L.; Investigation, Z.Z.; Writing—original draft, Z.Z., H.X., Y.X. and K.L. All authors have read and agreed to the published version of the manuscript.

Funding: This research was funded by the Key Laboratory of Quark and Lepton Physics (MOE) in Central China Normal University (No. QLPL2024P01), the China Scholarship Council (No. 202408420279), the NSFC Key Grant 12061141008, and the Scientific Research Foundation of Hubei University of Education for Talent Introduction (No. ESRC20230002).

Data Availability Statement: Data available in a publicly accessible repository. The original data presented in the study are openly available in hepdata at doi:10.17182/hepdata.71310.

Acknowledgments: The authors appreciate the referee for their careful reading of the paper and for their valuable comments.

Conflicts of Interest: The authors declare no conflicts of interest.

References

1. Arsene, I.; Bearden, I.G.; Beavis, D.; Besliu, C.; Budick, B.; Bøggild, H.; Chasman, C.; Christensen, C.H.; Christiansen, P.; Cibor, J.; et al. Quark gluon plasma and color glass condensate at RHIC? The Perspective from the BRAHMS experiment. *Nucl. Phys. A* **2005**, *757*, 1–27. [\[CrossRef\]](#)
2. Adcox, K.; Adler, S.S.; Afanasiev, S.; Aidala, C.; Ajitan, N.N.; Akiba, Y.; Al-Jamel, A.; Alexander, J.; Amirikas, R.; Aoki, K.; et al. Formation of dense partonic matter in relativistic nucleus-nucleus collisions at RHIC: Experimental evaluation by the PHENIX collaboration. *Nucl. Phys. A* **2005**, *757*, 184–283. [\[CrossRef\]](#)
3. Back, B.; Baker, M.D.; Ballintijn, M.; Barton, D.S.; Becker, B.; Betts, R.R.; Bickley, A.A.; Bindel, R.; Budzanowski, A.; Busza, W.; et al. The PHOBOS perspective on discoveries at RHIC. *Nucl. Phys. A* **2005**, *757*, 28–101. [\[CrossRef\]](#)
4. Adams, J.; Aggarwal, M.M.; Ahammed, Z.; Amonett, J.; Anderson, B.D.; Arkhipkin, D.; Averichev, G.S.; Badyal, S.K.; Bai, Y.; Balewski, J.; et al. Experimental and theoretical challenges in the search for the quark gluon plasma: The STAR Collaboration's critical assessment of the evidence from RHIC collisions. *Nucl. Phys. A* **2005**, *757*, 102–183. [\[CrossRef\]](#)
5. Aamodt, K.; Abelev, B.; Abrahantes Quintana, A.; Adamova, D.; Adare, A.M.; Aggarwal, M.M.; Aglieri Rinella, G.; Agocs, A.G.; Aguilar Salazar, S.; Ahammed, Z.; et al. Elliptic flow of charged particles in Pb-Pb collisions at 2.76 TeV. *Phys. Rev. Lett.* **2010**, *105*, 252302. [\[CrossRef\]](#)
6. ALICE Collaboration. Suppression of Charged Particle Production at Large Transverse Momentum in Central Pb-Pb Collisions at $\sqrt{s_{NN}} = 2.76 \text{ TeV}$. *Phys. Lett. B* **2011**, *696*, 30–39. [\[CrossRef\]](#)

7. Abelev, B.; Adam, J.; Adamová, D.; Adare, A.M.; Aggarwal, M.M.; Aglieri Rinella, G.; Agocs, A.G.; Agostinelli, A.; Aguilar Salazar, S.; Ahammed, Z.; et al. *J/ψ* suppression at forward rapidity in Pb-Pb collisions at $\sqrt{s_{NN}} = 2.76$ TeV. *Phys. Rev. Lett.* **2012**, *109*, 072301. [[CrossRef](#)]
8. ATLAS Collaboration. Observation of a Centrality-Dependent Dijet Asymmetry in Lead-Lead Collisions at $\sqrt{s_{NN}} = 2.77$ TeV with the ATLAS Detector at the LHC. *Phys. Rev. Lett.* **2010**, *105*, 252303. [[CrossRef](#)] [[PubMed](#)]
9. Chatrchyan, S.; Khachatryan, V.; Sirunyan, A.M.; Tumasyan, A.; Adam, W.; Bergauer, T.; Dragicevic, M.; Erö, J.; Fabjan, C.; Friedl, M.; et al. Observation and studies of jet quenching in PbPb collisions at nucleon-nucleon center-of-mass energy = 2.76 TeV. *Phys. Rev. C* **2011**, *84*, 024906. [[CrossRef](#)]
10. ALICE Collaboration. Centrality Dependence of Charged Particle Production at Large Transverse Momentum in Pb-Pb Collisions at $\sqrt{s_{NN}} = 2.76$ TeV. *Phys. Lett. B* **2013**, *720*, 52–62. [[CrossRef](#)]
11. Braun-Munzinger, P.; Koch, V.; Schäfer, T.; Stachel, J. Properties of hot and dense matter from relativistic heavy ion collisions. *Phys. Rep.* **2016**, *621*, 76–126. [[CrossRef](#)]
12. Adamczyk, L.; Adkins, J.K.; Agakishiev, G.; Aggarwal, M.M.; Ahammed, Z.; Ajitanand, N.N.; Alekseev, I.; Anderson, D.M.; Aoyama, R.; Aparin, A.; et al. Bulk properties of the medium produced in relativistic heavy-ion collisions from the beam energy scan program. *Phys. Rev. C* **2017**, *96*, 044904. [[CrossRef](#)]
13. Adam, J.; ALICE Collaboration; Adamová, D.; Aggarwal, M.M.; Aglieri Rinella, G.; Agnello, M.; Agrawal, N.; Ahammed, Z.; Ahn, S.U.; Aimo, I.; et al. Centrality dependence of the nuclear modification factor of charged pions, kaons, and protons in Pb-Pb collisions at $\sqrt{s_{NN}} = 2.76$ TeV. *Phys. Rev. C* **2016**, *93*, 034913. [[CrossRef](#)]
14. Fazzini, T.; Fidecaro, G.; Merrison, A.W.; Paul, H.; Tollestrup, A.V. Electron Decay of the Pion. *Phys. Rev. Lett.* **1958**, *1*, 247–249. [[CrossRef](#)]
15. Ambrosino, F.; Antonelli, A.; Antonelli, M.; Archilli, F.; Bacci, C.; Beltrame, P.; Bencivenni, G.; Bertolucci, S.; Bini, C.; Bloise, C.; et al. Measurement of the charged kaon lifetime with the KLOE detector. *J. High Energy Phys.* **2008**, *2008*, 073.
16. Sjöstrand, T.; Mrenna, S.; Skands, P. PYTHIA 6.4 physics and manual. *J. High Energy Phys.* **2006**, *05*, 026. [[CrossRef](#)]
17. Arsene, I.; Bearden, I.G.; Beavis, D.; Besliu, C.; Budick, B.; Bøggild, H.; Chasman, C.; Christensen, C.H.; Christensen, P.; Cibor, J.; et al. Evolution of the nuclear modification factors with rapidity and centrality in d+Au collisions at $\sqrt{s_{NN}} = 200$ GeV. *Phys. Rev. Lett.* **2004**, *93*, 242303. [[CrossRef](#)]
18. Milov, A.; ATLAS Collaboration. Centrality dependence of charged particle spectra and RCP in Pb + Pb collisions at $\sqrt{s_{NN}} = 2.76$ TeV with the ATLAS detector at the LHC. *J. Phys. G Nucl. Part. Phys.* **2011**, *38*, 124113. [[CrossRef](#)]
19. ALICE Collaboration. Production of muons from heavy-flavour hadron decays at high transverse momentum in Pb-Pb collisions at $\sqrt{s_{NN}} = 5.02$ and 2.76 TeV. *Phys. Lett. B* **2021**, *820*, 136558. [[CrossRef](#)]
20. ALICE Collaboration. *Technical Design Report for the Muon Forward Tracker*; Technical Report; CERN-LHCC-2015-001; ALICETDR-018; ALICE Collaboration: Geneva, Switzerland, 2015.
21. Acharya, S.; Adamová, D.; Adhya, S.P.; Adler, A.; Adolfsson, J.; Aggarwal, M.M.; Rinella, G.A.; Agnello, M.; Agrawal, N.; Ahammed, Z.; et al. Production of muons from heavy-flavour hadron decays in pp collisions at $\sqrt{s} = 5.02$ TeV. *J. High Energy Phys.* **2019**, *2019*, 8. [[CrossRef](#)]
22. ALICE Collaboration. Production of muons from heavy-flavour hadron decays in p-Pb collisions at $\sqrt{s_{NN}} = 5.02$ TeV. *Phys. Lett. B* **2017**, *770*, 459–472. [[CrossRef](#)]
23. ALICE Collaboration. Inclusive heavy-flavour production at central and forward rapidity in Xe-Xe collisions at $\sqrt{s_{NN}} = 5.44$ TeV. *Phys. Lett. B* **2021**, *819*, 136437. [[CrossRef](#)]

Disclaimer/Publisher’s Note: The statements, opinions and data contained in all publications are solely those of the individual author(s) and contributor(s) and not of MDPI and/or the editor(s). MDPI and/or the editor(s) disclaim responsibility for any injury to people or property resulting from any ideas, methods, instructions or products referred to in the content.